

# Non-universality of scaling exponents in quantum Hall transitions

N A Dadoo-Amoo, K Saeed, D Mistry, S P Khanna, L Li, E H Linfield, A G Davies and J E Cunningham

School of Electronic and Electrical Engineering, University of Leeds, Woodhouse Lane, Leeds, LS2 9JT, UK

E-mail: [eenjec@leeds.ac.uk](mailto:eenjec@leeds.ac.uk)

Received 9 May 2014, revised 29 September 2014

Accepted for publication 3 October 2014

Published 29 October 2014

## Abstract

We have investigated experimentally the scaling behaviour of quantum Hall transitions in GaAs/AlGaAs heterostructures of a range of mobility, carrier concentration, and spacer layer width. All three critical scaling exponents  $\gamma$ ,  $\kappa$  and  $p$  were determined independently for each sample. We measure the localization length exponent to be  $\gamma \approx 2.3$ , in good agreement with expected predictions from scaling theory, but  $\kappa$  and  $p$  are found to possess non-universal values. Results obtained for  $\kappa$  range from  $\kappa = 0.16 \pm 0.02$  to  $\kappa = 0.67 \pm 0.02$ , and are found to be Landau level (LL) dependent, whereas  $p$  is found to decrease with increasing sample mobility. Our results demonstrate the existence of two transport regimes in the LL conductivity peak; universality is found within the quantum coherent transport regime present in the tails of the conductivity peak, but is absent within the classical transport regime found close to the critical point at the centre of the conductivity peak. We explain these results using a percolation model and show that the critical scaling exponent depends on certain important length scales that correspond to the microscopic description of electron transport in the bulk of a two-dimensional electron system.

Keywords: quantum Hall effect, localization, scaling

(Some figures may appear in colour only in the online journal)

## 1. Introduction

The behaviour of the electron wave functions at the centre of Landau levels (LLs) in the integer quantum Hall effect (IQHE) regime is understood to be a result of continuous quantum phase transitions between localized and delocalized (extended) energy states in two-dimensional electron systems (2DESs) [1]. The IQHE, which occurs in 2DESs in a strong perpendicular magnetic field [2], is characterized by plateaux in the Hall conductivity  $\sigma_{xy}$  (precisely quantized in integer multiples of  $e^2/h$ ) with a simultaneous vanishingly small diagonal conductivity  $\sigma_{xx}$ . LLs occur when a perpendicular magnetic field is applied to a 2DES, which breaks the continuous 2D density of states into discrete energy levels.

Impurity scattering and crystal inhomogeneities produce disorder potentials that broaden the LLs into energy bands, in which the states at the centres of the LLs are extended and all other states are localized. Plateaux in  $\sigma_{xy}$  occur when the Fermi energy lies in the regions of localized states, while plateau-to-plateau transitions (PPTs) occur when the Fermi energy moves through the delocalized states.

A critical behaviour of the electron wave functions is observed at these transitions between quantized Hall plateaux. This critical behaviour in 2DESs is governed by a diverging localization length

$$\xi \propto |E - E_c|^{-\gamma}. \quad (1)$$

$\xi$  scales as the critical energy  $E_c$  as the LL centre is approached, where  $\gamma$  is the critical localization length exponent. Since the LL energy can be controlled by changing the magnetic field, equation (1) can also be expressed as  $\xi \propto |B - B_c|^{-\gamma}$ ,



Content from this work may be used under the terms of the [Creative Commons Attribution 3.0 licence](https://creativecommons.org/licenses/by/3.0/). Any further distribution of this work must maintain attribution to the author(s) and the title of the work, journal citation and DOI.

where  $B_c$  is a critical magnetic field. As with all continuous phase transitions, the value of the critical exponent is expected to be a universal constant [3]. The localization length exponent is predicted to be approximately  $\gamma \approx 2.35$  [3–5], independent of LL index and the correlation length of the disorder potentials. According to finite size scaling theory [3, 4, 6], a temperature dependence of the slope of the plateau transition, or equivalently of the width of the  $\sigma_{xx}$  peak, can be observed.

At low and finite temperatures the effective system size  $L$  is given by the quantum phase coherence length [4, 7]

$$L \propto T^{-p/2}. \quad (2)$$

As the temperature approaches zero the effective length can be expressed as  $L^{1/\gamma} \propto T^{-\kappa}$  where  $\kappa = p/2\gamma$ .  $\kappa$  and  $p$ , like  $\gamma$ , are expected to possess universal values of  $\kappa = 0.42$  and  $p = 2$  according to the scaling theory of the IQHE [4–6]. The conductivity tensor reflects a single-scaling parameter scaling for both  $\sigma_{xy}$  and  $\sigma_{xx}$  [6] that depends on  $T$  and  $B$ . The conductivity components can be shown [4, 6] to be

$$\sigma_{\mu\nu}(TB) = S_{\mu\nu}[L^{1/\gamma}|B - B_c|]. \quad (3)$$

The derivative of (3) at the critical field  $B_c$  provides direct experimental access to the critical exponents,

$$\frac{d\sigma_{\mu\nu}(B_c)}{dB} \propto L^{1/\gamma} \propto T^{-\kappa}, \quad (4)$$

which can be expressed as  $(d\sigma_{xy}/dB)_{\max} \propto T^{-\kappa}$  using the maximum slope of the Hall conductivity transition, or  $\Delta B_{\sigma_{xx}} \propto T^\kappa$  using the width of the diagonal conductivity peak.

The nature of QHE transitions has for some time been of interest to both experimentalists and theorists. Though the physics of the QHE has been studied extensively over the years, the nature of PPT still remains unclear. In particular, the question of the universality of the divergent  $\xi$  has been disputed by several experimental results and has created some disagreement both in the experimental and in the theoretical literature [4, 8–23]. The first experimental measurements of the critical exponent  $\kappa$  were performed on electrons confined in InGaAs/InP heterostructures using equation (4) above, where it was found that  $\kappa = 0.42$  [11], independent of sample properties or LL index, and in remarkable agreement with the theoretically expected universal value. This result has been supported by subsequent InGaAs/InP measurements where it was confirmed that  $\kappa = 0.42$  [24], further strengthening the argument for universality in InGaAs/InP heterostructures. Similar measurements on GaAs/AlGaAs heterostructures using the same analysis did not, however, yield universal values [9, 14, 21], with some results suggesting a dependence of  $\kappa$  on the impurity scattering strength [9]. Other measurements on GaAs/AlGaAs heterostructures failed even to support the power law form described above, but rather suggested a linear dependence of the scaling of PPTs [17, 20].

Experimental measurements of  $\gamma$  have also been analysed by using a size-dependent scaling analysis [8], and variable-range hopping theory [14, 25] on 2DESs formed in GaAs/AlGaAs heterostructures. Both analyses found  $\gamma$  to be

universal. All work performed on InGaAs/InP based samples has inferred values of  $\gamma$  from measurements of  $\kappa$ , assisted by the assumption that  $p = 2$ , but no work has attempted a direct evaluation of  $\gamma$ .

Measurements of  $p$  at PPTs of InGaAs/InP heterostructures using a current scaling technique through electron heating [26] also found universal values. Though size-dependent measurements have been used to extract  $p$  in GaAs/AlGaAs heterostructures, there still remains a lack of a direct measurement of  $p$  at the PPT in GaAs/AlGaAs heterostructures. The size-dependent scaling method, however, did not produce universal values [8]. In experiments where  $p$  is not measured, it is generally assumed that  $p = 2$  but this assumption is disputed by some authors [18], where it is argued that there is no justification for using the clean limit result of  $p = 2$  rather than the disordered result of  $p = 1$ .

In summary, measurements of  $\kappa$  and  $p$  in InGaAs/InP heterostructures have shown universal values, while those of GaAs/AlGaAs heterostructures have not, whereas measurements of  $\gamma$  have shown universal values in GaAs/AlGaAs heterostructures, but have not been made in InGaAs/InP heterostructures.

It has long been argued [4], and indeed recently observed [27, 28], that the presence or absence of universality in a particular heterostructure is affected by the correlation length of disorder (the range of the disorder potentials) in the sample. Electrons confined in InGaAs/InP heterostructures predominantly experience alloy-disorder scattering within the vicinity of the 2DES, making the correlation length of the disorder potential relatively short-ranged. For 2DESs formed in GaAs/AlGaAs heterostructures, scattering processes are usually dominated by ionized impurities in the donor layer, which are separated from the 2DES by a spacer layer which makes the correlation length of the disorder potential relatively long-ranged. Though the results from these disorder-based experiments have shed new light on the universality problem, questions still remain about the conditions required for the observation of universal quantum criticality. We will show below that the range of the disorder potential is not itself sufficient to explain all the discrepancies observed in critical scaling exponents of PPTs.

It is not obvious that a complete and robust picture of the quantum criticality of PPT can be found by combining direct and indirect evaluations of critical exponents obtained from different samples in different materials systems. There is a need for a converging experiment where all three exponents are measured in the same system; this would allow direct comparisons between scaling exponents to be made with confidence, this is the central aim of the current work. In this paper we evaluate all three scaling exponents ( $\kappa$ ,  $p$  and  $\gamma$ ) *in the same samples* through direct and independent measurements across a range of four GaAs/AlGaAs heterostructures. This materials system was chosen as it is in this system where the greatest degree of disagreement in scaling exponents has been found previously. We show experimentally that the universality of scaling exponents depends intrinsically on key length scales that determine the regime of 2DES transport. Based on our results, we provide a broader definition of

**Table 1.** Wafer layer and electrical characteristics measured at 100 mK without illumination.

Sample	AlGaAs spacer (nm)	$n_e$ ( $\times 10^{11}$ cm $^{-2}$ )	$\mu_e$ ( $\times 10^5$ cm $^2$ V $^{-1}$ s $^{-1}$ )
L1	20	2.99	3.8
L2	40	1.55	1.09
L3	20	2.45	0.51
L4	40	1.92	8.68

quantum critically in PPTs through a percolation model that is consistent both with our experimental results and with those from other groups. The model also accounts for the generally accepted correlation length of disorder argument which is used to explain the discrepancy in universality between short-range and long-range disordered systems [4]. In particular, we are able to answer the question of whether both critical exponents  $\gamma$  and  $p$  are non-universal if  $\kappa$  is determined to be non-universal in a system, noting that  $\kappa$  is a composite exponent,  $\kappa = p/2\gamma$ , which depends on two independent exponents.

The paper is structured as follows. Experimental techniques and details of the samples used are given in section 2. The analysis and results for the three exponents are presented in section 3. Section 4 discusses the percolation model, which is used to explain our results. Section 5 comprises a discussion of the results and the implications for the universality of scaling in the QHE. Conclusions are summarized in section 6.

## 2. Sample properties and experimental technique

All samples were fabricated from GaAs/AlGaAs wafers grown by molecular beam epitaxy. Four different heterostructures were grown, as summarized in table 1, to provide a range of mobilities, carrier concentrations, and spacer layer thicknesses. The growth sequence of the wafers (from substrate to surface) was: an undoped 1- $\mu$ m-thick GaAs layer; an undoped Al $_{0.33}$ Ga $_{0.67}$ As spacer (either 20 or 40 nm thick); a 40 nm Si-doped ( $2 \times 10^{18}$  cm $^{-3}$ ) Al $_{0.33}$ Ga $_{0.67}$ As layer; and a 10 nm GaAs cap layer. The samples were patterned using optical lithography to form Hall bars with a channel width of 100  $\mu$ m and length of 300  $\mu$ m between the voltage probe arms.

Low resistance ohmic contacts were prepared by evaporating 170 nm of Au/Ge/Ni eutectic onto the surface of the Hall bar, which was then annealed at 430  $^{\circ}$ C for 80 s under a nitrogen atmosphere. The samples were attached to the mixing chamber plate of a  $^3$ He/ $^4$ He dilution refrigerator, and simultaneous measurements of the diagonal ( $\rho_{xx}$ ) and Hall ( $\rho_{xy}$ ) resistivities were taken between 0.1 and 1 K using standard low-frequency (7 Hz) lock-in techniques.

It was determined that the samples were not heated by excitation currents below 50 nA, and so a fixed 10 nA input current was used for all temperature scaling measurements involving  $\kappa$  and  $\gamma$ . The excitation current was varied for measurements of  $p$ , however, with current heating purposely used (see section 3). Figure 1 shows a plot of  $\rho_{xx}$  and  $\rho_{xy}$  as a function of magnetic field at different temperatures for one sample. The temperature dependence of the QHE can clearly

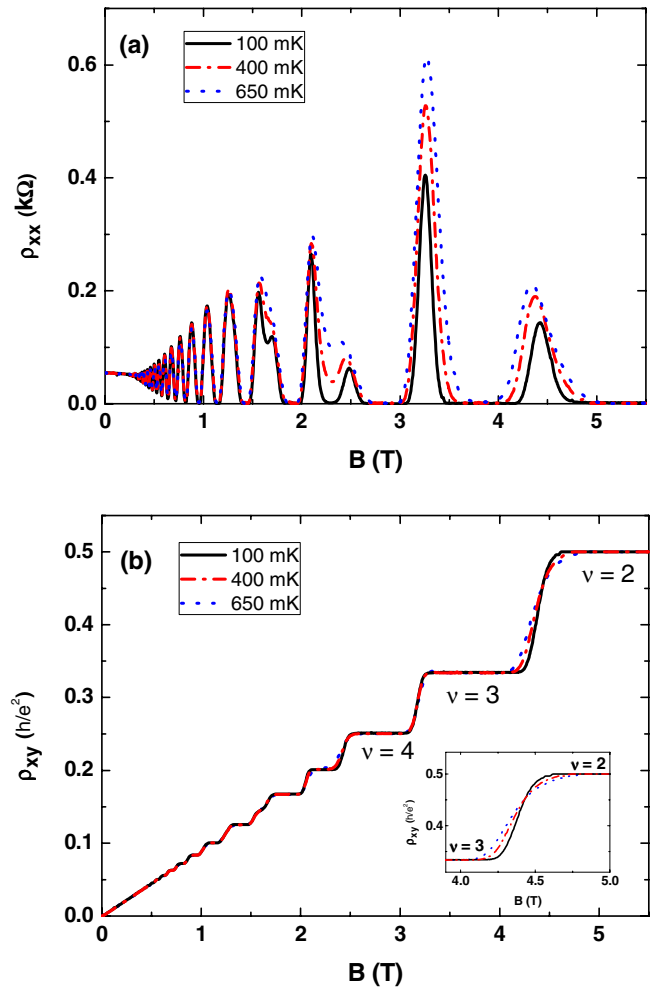


**Figure 1.** (a)  $\rho_{xx}$  measured at different temperatures for sample L1 with an excitation current of 10 nA. (b) The corresponding Hall resistivity  $\rho_{xy}$  and filling factor,  $\nu$ . Inset:  $\nu = 3-2$  PPT.

be seen in figure 1; the peaks in the longitudinal resistivity broaden with increasing temperature, while the slope of the PPTs in the Hall resistivity decreases with increasing temperature.

## 3. Experimental results

### 3.1. The localization length exponent, $\gamma$

If the energy separation between disorder broadened LLs is much greater than their linewidth, then the states in the LL tails are considered to be localized [29]. The localization length  $\xi$  is expected to diverge as the Fermi energy approaches the centre of the LL (equation (1)), and this divergence yields the scaling exponent  $\gamma$ . Numerical and analytical studies have predicted a universal value of  $\gamma \approx 2.35$  [4, 5, 12, 30–32], which has been experimentally validated [8, 14, 25, 33]. The first experimental measurement of  $\gamma$  was based on a size-dependent scaling theory [8]. This theory assumes that  $\xi(E_F)$  is limited by the physical dimensions of the sample, which creates a low temperature saturation limit beyond which  $\xi$  is pinned at the sample size  $W$ . By measuring the  $\sigma_{xx}$  peak width

within the saturated region for samples of different sizes,  $\gamma$  can be determined through  $W \propto \xi_{\text{sat}} \propto \Delta B^{-\gamma}$ . We use a different and more direct approach to determine  $\gamma$ , however, which relies on a direct evaluation of  $\xi$  and its energy dependence through variable-range hopping theory [34].

At sufficiently low temperatures, the dominant transport mechanism in the localized region of an energy band is variable-range hopping (VRH) [29], where the temperature dependence of  $\sigma_{xx}$  can be described by

$$\sigma_{xx}(T) \propto e^{-(T_0/T)^\alpha}, \quad (5)$$

where  $T_0$  is the characteristic hopping temperature. Equation (5) was initially conceived to describe Mott hopping with  $\alpha = \frac{1}{1+d}$ , where  $d$  refers to the dimensionality of the system [29, 35]. Upon further investigation of hopping conductivity in disordered systems, it was found that the Coulomb interaction between localized electrons creates a Coulomb gap in the density of states near the Fermi level [36].

At low temperatures, the influence of the Coulomb gap modifies the exponent of the hopping conductivity to  $\alpha = 1/2$  in two dimensions [36],

$$\sigma_{xx}(T) = \sigma_0 e^{-(T_0/T)^{1/2}}, \quad (6)$$

where

$$k_B T_0 = C \frac{e^2}{4\pi\epsilon_r\epsilon_0\xi}, \quad (7)$$

and  $\sigma_0$  is a prefactor that is inversely proportional to temperature ([23, 37–39]. The dimensionless constant  $C$  is thought to be of the order of unity and is believed to be  $C \approx 6$  [25] in two dimensions. Ono [40] independently derived the temperature-dependent  $\sigma_{xx}$  relationship in equation (5) in the tail states of a LL and also found  $\alpha = 1/2$  (from equation (5)) in two-dimensions and a prefactor similarly inversely proportional to temperature. Our data, as shown in figure 2(b), was tested within the localized region with different values of  $\alpha$ , and the best fit was found to be  $\alpha = 1/2$ .

From equations (1), (6) and (7) a direct relationship can be found between  $\xi$  and VRH that allows  $\gamma$  to be measured.  $\xi$ , which is inversely proportional to  $T_0$ , can be experimentally measured by determining  $T_0$  from a double log plot of  $T\sigma_{xx}$  versus  $1/T^{1/2}$  according to equation (6). Figure 2(b) shows  $T_0$  determined at different points away from the critical field of the  $\sigma_{xx}$  peak shown in figure 2(a); it can be seen that VRH fits our data well over a wide range of filling factors ( $|\delta\nu| \approx 0.4$ ), deep into the tails of the broadened LL band. By determining  $T_0$  as a function of magnetic field away from the critical field,  $|\delta B|$ , we determine the localization length exponent  $\gamma$  by the gradient of a linear fit to  $\ln(T_0) = \gamma \ln(\delta B)$  as shown in figure 3 for all four heterostructures investigated. The values of  $\gamma$  obtained are summarized in table 2; two values of  $\gamma$  are obtained for the  $N = 1 \downarrow$  LL (4–3 transition) in each sample, one for the high- $B$  side of the LL, and one for the low- $B$  side.  $N = 1 \downarrow$  LL was chosen for investigation as it did not exhibit LL coupling or spin-orbit interaction in our samples, since the presence of these effects is expected to change the measured value of  $\gamma$  [4]. The values obtained for all four of our samples are in good agreement with the

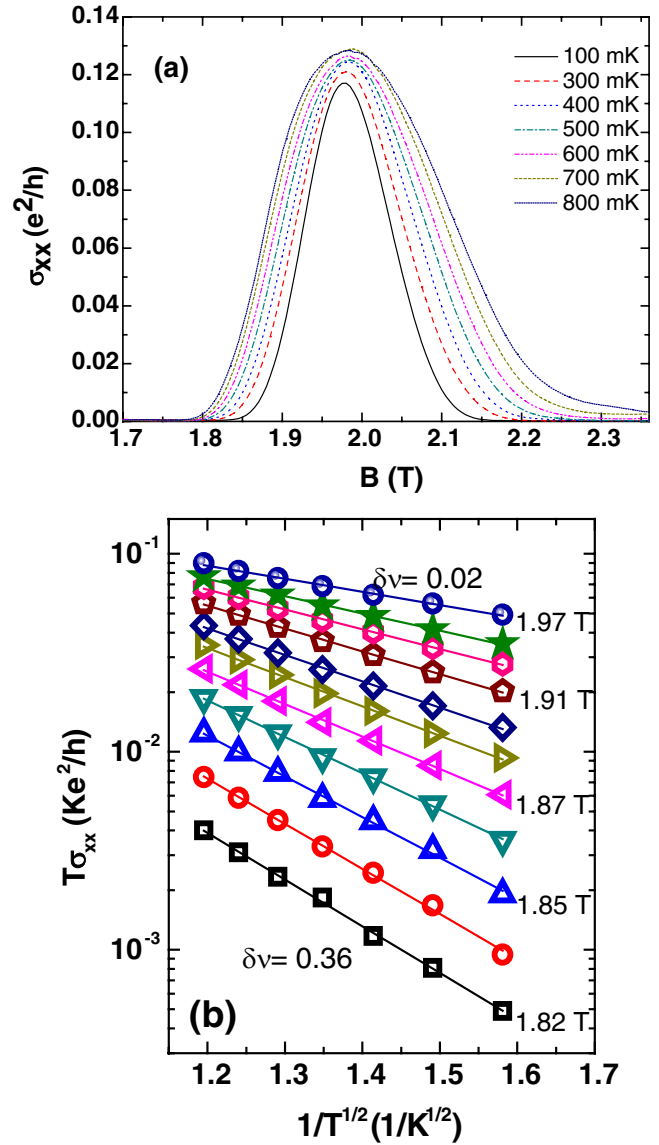


**Figure 2.** (a) Temperature dependence of the  $\nu = 4-3$  transition peak for sample L4. The peak width increases with temperature. (b) Semi-log plot of the temperature dependence of  $\sigma_{xx}$  taken from the data in (a), using equation (5).

expected universal value of  $\gamma \approx 2.3$  with the exception of L3, in which  $\gamma$  was found to be  $\gamma = 1.79 \pm 0.01$  on the high- $B$  side. This discrepancy is attributed to the strong onset of LL coupling between the  $N = 1 \downarrow$  and  $N = 1 \uparrow$  LLs with increasing temperature, caused by the relatively high level of disorder in this particular heterostructure as suggested by its comparatively low mobility (see table 1). The inset to figure 3(c) shows that for sample L3 the LLs represented by the two  $\sigma_{xx}$  peaks are not distinguishably separated, and so  $\gamma$  could not be accurately determined on the high- $B$  side of the  $N = 1 \downarrow$  LL. LL coupling was not observed in the other three heterostructures; the figure 3(a) inset shows distinguishable LLs in sample L1, for example, indicating negligible LL coupling.

Assuming  $C = 6.2$  [25] and using  $\epsilon_r \approx 12.6$  for GaAs, in all our samples the localization length was consistently found to be  $\xi \approx 3\mu\text{m}$  approaching the critical point at the LL centres,

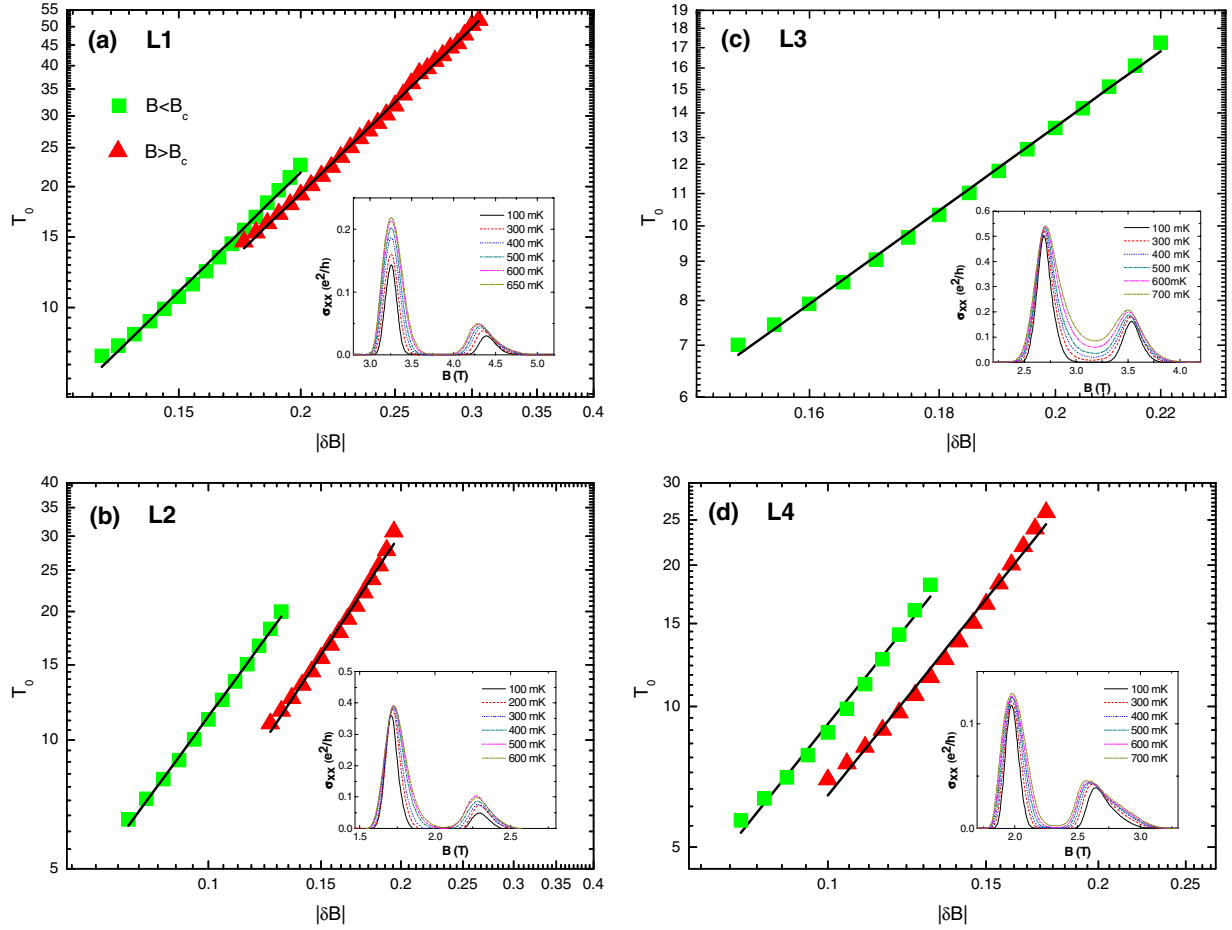


**Figure 3.** Logarithmic plot of  $T_0$  as a function of distance in magnetic field away from the critical point,  $\delta B$ , for the  $N = 1 \downarrow$  LL.  $\gamma$  is measured as the gradient of the linear fit to  $\ln(T_0) = \gamma \ln(\delta B)$ .  $\gamma$  is determined for all four samples investigated,  $\blacksquare$  represents measurements taken on the low- $B$  side of the critical point, while  $\blacktriangle$  represents measurements on the high- $B$  side. The values determined are in good agreement with the expected value of  $\gamma \approx 2.3$ . The insets show  $\sigma_{xx}(B)$  as a function of temperature for all samples; strong temperature-dependent LL coupling is observed in sample L3 preventing the determination of  $\gamma$  for the high- $B$  sided of the LL.

**Table 2.** The localization length exponent  $\gamma$ , measured for the  $N = 1 \downarrow$  LL. Two values of  $\gamma$  are determined from measurements of each sample, one from the low field side of the peak and the other from the high field side.

Sample	$N = 1 \downarrow$	
	$B < B_c$	$B > B_c$
L1	$2.37 \pm 0.05$	$2.34 \pm 0.02$
L2	$2.05 \pm 0.03$	$2.28 \pm 0.05$
L3	$2.36 \pm 0.03$	$1.79 \pm 0.01$
L4	$2.39 \pm 0.08$	$2.39 \pm 0.06$

and  $\xi \approx 200$  nm as the ends of the LL tails were approached (equation (7)). This is much smaller than the sample size, suggesting strong localization in the tail regions of the LL. These values are consistent with similar measurements on devices of similar size [25, 41].

### 3.2. Temperature scaling exponent, $\kappa$

The exponent  $\kappa$  has been the most frequently investigated scaling exponent. Following the prediction of a universal scaling behaviour by Pruisken [6], Wei *et al* conducted

temperature-dependent measurements on the IQHE in a InGaAs/InP 2DES [11] and found that the transition region between plateaux exhibits a scaling behaviour in the form of the power laws:

$$(d\rho_{xy}/dB)_{\max} \propto T^{-\kappa}, \quad (8)$$

and,

$$\Delta B_{xx} \propto T^\kappa, \quad (9)$$

where equation (8) refers to the maximum of the derivative of the Hall resistivity  $\rho_{xy}$  between PPTs, and equation (9) measures the width of the peak in  $\rho_{xx}$  between adjacent plateaux. The result of these investigations yielded a universal scaling exponent  $\kappa = 0.42 \pm 0.02$  from both equations (8) and (9). Subsequent investigations have questioned the universality of  $\kappa$ , however. Investigations on GaAs/AlGaAs heterostructures [10] found  $\kappa$  to be universal only below a characteristic temperature of 200 mK, which was attributed to the dominance of long-range potential fluctuations in GaAs/AlGaAs heterostructures. Koch *et al* [9] also investigated  $\kappa$  in GaAs/AlGaAs, and found  $\kappa$  to be mobility dependent. Studies in Si-MOSFETs [43, 44] also failed to observe universality in the exponent  $\kappa$ . Furthermore, a similar

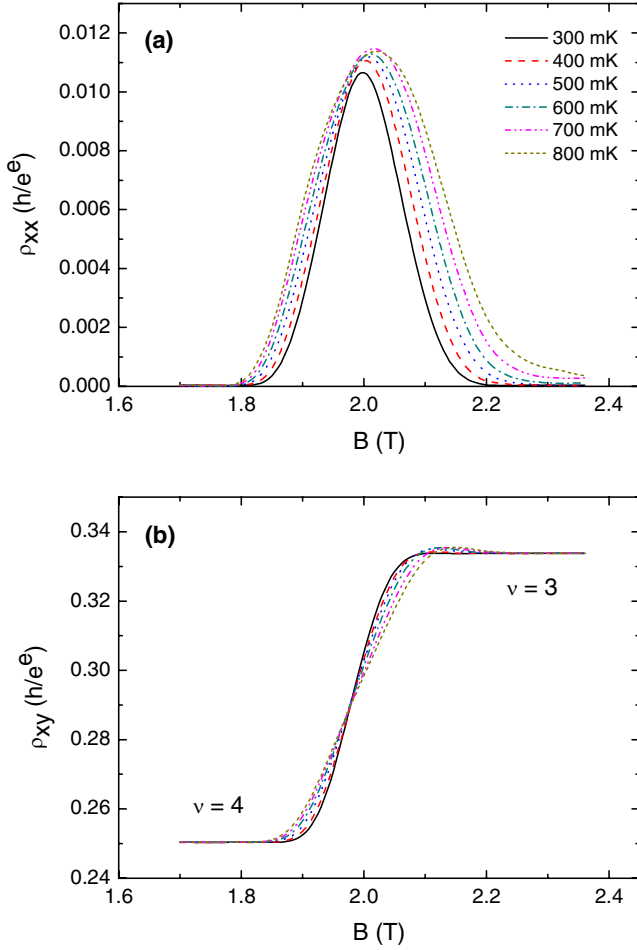


**Figure 4.** (a)  $\rho_{xx}$  and (b)  $\rho_{xy}$  for the  $N = 1 \downarrow$  ( $\nu = 4-3$ ) transition as a function of magnetic field at series of different temperatures for sample L4.

dependence is expected in measurement frequency according to equation (8) and (9) [3, 4], but there is no consensus on a universal  $\kappa$  in such frequency scaling experiments either [16, 17, 42]. As discussed above, the scaling exponent  $\gamma$  is universal in all our samples. In this section we measure  $\kappa$  in the same set of samples and investigate its universality. We determine  $\kappa$  for the  $\nu = 4-3$  and  $\nu = 3-2$  transitions using both equations (8) and (9). Figure 4 shows an example of  $\rho_{xy}$  and  $\rho_{xx}$  for the  $\nu = 4-3$  transition about the  $N = 1 \downarrow$  LL for one of our samples.

Figure 5 shows plots used to determine  $\kappa$  based on equation (9) for the  $N = 1 \downarrow$  and  $N = 1 \uparrow$  LLs. Our results are summarized in table 3. In general the results from equations (8) and (9) agree well with each other. Our results do not show a general universal behaviour, but we note that the values for  $\kappa$  in  $N = 1 \uparrow$  are closely distributed about the predicted universal value of  $\kappa \approx 0.42$ .

### 3.3. Temperature scattering exponent, $p$

Although there have been a number of investigations of the critical scaling exponents of the QHE, experimental measurements of  $p$  near the critical field, and independent of other critical exponents, are the least studied. We present here

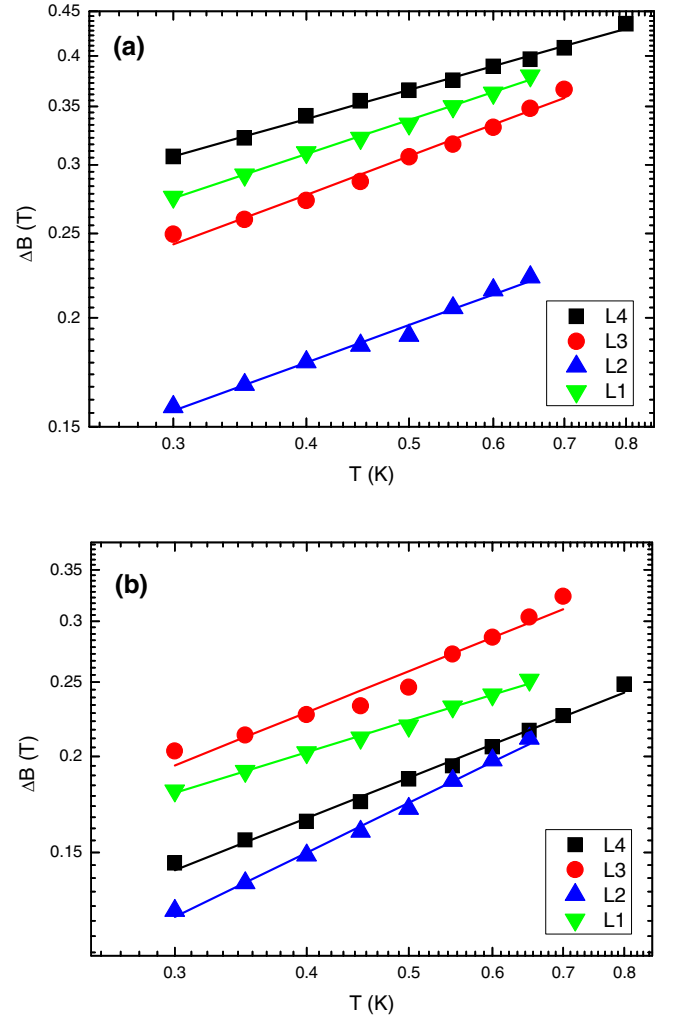


**Figure 5.** (a)  $\Delta B_{xx}$  versus  $T$  for the  $N = 1 \uparrow$  ( $\nu = 3-2$ ) transition for all four samples investigated. (b)  $\Delta B_{xx}$  versus  $T$  for the  $\nu = 4-3$  transition.

**Table 3.** The exponent  $\kappa$  measured for LLs  $N = 1 \downarrow$  ( $\nu = 4-3$  transition) and  $N = 1 \uparrow$  ( $\nu = 3-2$  transition) using both the width of the transition peaks,  $\Delta B_{xx}$ , determined from the full-width-at-half-maximum of the normalized resistivity traces, and the maximum gradient of plateau transitions,  $d\rho_{xy}/dB$ .

Sample	$N = 1 \downarrow$		$N = 1 \uparrow$	
	$\Delta B_{xx}$	$d\rho_{xy}/dB$	$\Delta B$	$d\rho_{xy}/dB$
L1	$0.42 \pm 0.01$	$0.23 \pm 0.02$	$0.41 \pm 0.01$	$0.44 \pm 0.02$
L2	$0.67 \pm 0.02$	$0.66 \pm 0.03$	$0.44 \pm 0.02$	$0.42 \pm 0.03$
L3	$0.55 \pm 0.04$	$0.60 \pm 0.02$	$0.46 \pm 0.02$	$0.43 \pm 0.03$
L4	$0.54 \pm 0.02$	$0.54 \pm 0.02$	$0.34 \pm 0.01$	$0.16 \pm 0.02$

an independent determination of the temperature exponent of the inelastic scattering length,  $p$ .

The effective size of a 2DES is limited by a temperature-dependent inelastic scattering length. Thouless [7] showed that the inelastic scattering length introduces random fluctuations in electronic states that limit the quantum interference necessary for localization. In other words, if the inelastic scattering length is less than the localization length, the effects of localization will be destroyed since an electron

will be scattered before it is able to explore the length of the system. An electron with a lifetime  $\tau_{in}$  will diffuse a distance,

$$L^2 = D\tau_{in}, \quad (10)$$

where  $D$  is the diffusion constant for an electron.  $L$ , the Thouless length, describes the distance over which quantum coherence is maintained in the system; localization effects are cut off beyond this length. At sufficiently high temperatures, the quantum coherence length is determined by the temperature-dependent inelastic scattering length. An increase in temperature results in a decrease in the inelastic scattering length. This makes the elastic scattering length the relevant length scale for the observation of localization effects of quantum Hall transitions since at sufficiently high temperatures it is the limiting length of quantum coherence.

The temperature dependence of the inelastic scattering time can be expressed as  $\tau_{in} \propto T^{-p}$  where  $p$  is an exponent of temperature that depends on the scattering mechanism within the system. From equation (10) a scaling expression of the dependence of  $L$  on temperature can be written as

$$L \propto T^{-p/2}. \quad (11)$$

Equation (11) shows that the quantum coherent size of a system can be varied by changing the sample temperature. For all the experiments described above (involving the critical exponents  $\kappa$  and  $\gamma$ ), the system size of the 2DES has been effectively scaled by controlling the bath temperature, which determines the sample lattice temperature,  $T_L$ . In all our experiments, sufficient time is allowed to bring the lattice and bath temperature to equilibrium.

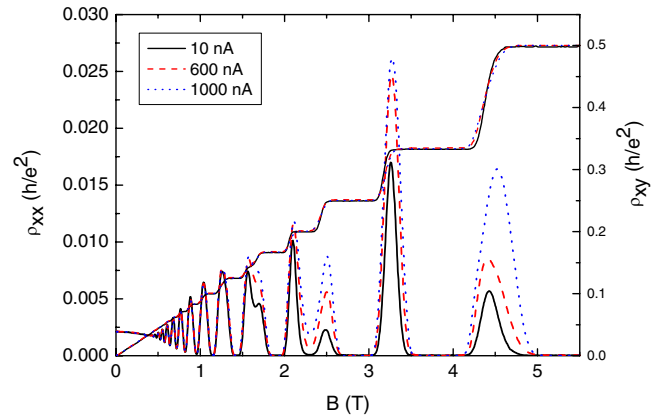
At high  $T_L$ , energy is easily transferred between electrons and the lattice with little temperature lag, and the electron temperature  $T_e$  in the 2DES is essentially  $T_e \approx T_L$ . At low  $T_L$ , electron–phonon interaction is weak, and it is possible for  $T_e$  to be much higher than  $T_L$  under an applied electric field. Anderson *et al* [45] proposed such an electron heating model and showed that within this weak electron–phonon coupling regime the field dependence of the electron temperature can be expressed as

$$\pi k_B T_e = 4eE(D\tau_{in})^{1/2}, \quad (12)$$

where  $E$  is the applied electric field and  $D$  is the diffusion constant. From equations (10), (11) and (12) the coefficient of the ratio of  $\ln E$  to that of  $\ln T$  is  $2/(2+p)$ . This can be expressed in terms of the applied current  $I$  as

$$T_e \propto I^\eta, \quad \text{where } \eta = \frac{2}{2+p}. \quad (13)$$

In previous investigations it has been shown that by comparing a change in resistivity as a function of temperature with the change in resistivity as a function of electric field or current, the electron temperature corresponding to a particular field, or current, can be extracted [46, 47]. It can be observed in equations (12) and (13) that through a combination of field or current dependent scaling experiments, where electrons in the 2DES are heated against a background of a constant and low lattice temperature, it is possible to determine  $p$  by measuring the sample resistivity as a function of the applied electric field.



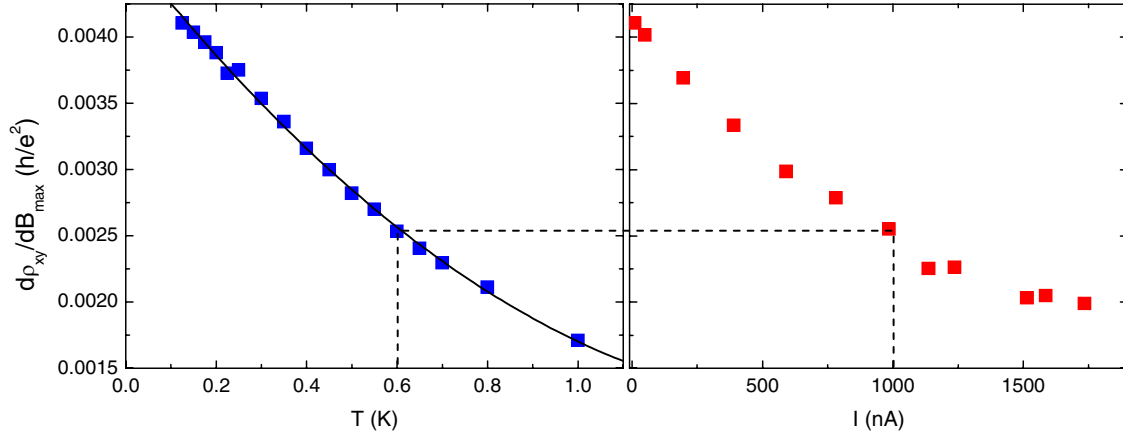
**Figure 6.** Diagonal and Hall resistivity measured with three different applied currents in sample L1. Electron heating is evident in the broadening of the peaks in the diagonal resistivity and the reduction in the inter-plateau slope of the Hall resistivity.

Figure 6, which is comparable to figure 1, shows evidence of electron heating with increasing current. We attribute the broadening of the peaks in the diagonal resistivity and the reduction in the slope of PPTs of the Hall resistivity in figures 1 and 6 to the same finite-size scaling mechanism [3, 48] in both temperature and current dependent cases, respectively.

The electron temperature here is determined through the temperature dependence of the  $d\rho_{xy}/dB$  maximum ( $d\rho_{xy}/dB_{max}$ ), which occurs at the critical point. The temperature dependence of  $d\rho_{xy}/dB_{max}$  is measured at different  $T_L$  while applying a low and constant current to ensure that there is negligible electron heating, and the results are used to create calibration curves for each transition of each sample. Similar measurements of  $d\rho_{xy}/dB_{max}$  are obtained by varying the applied currents. For each  $d\rho_{xy}/dB_{max}$  measured at a different applied current,  $T_e$  is determined using the corresponding calibration curve obtained from the temperature-dependent experiments. By comparing  $d\rho_{xy}/dB_{max}$  determined in both temperature and current scaling studies,  $T_e$  is derived for each measured current. Figure 7 shows such a comparison for the  $\nu = 4-3$  transition of sample L4, where an applied current of 1000 nA corresponds to  $T_e \sim 600$  mK. This method is similar to determination of electron temperature from the dampening of Shubnikov–de Haas oscillations with applied electric field or current [49–51]. Since critical scaling phenomena are of interest here, it is important that the determination of  $T_e$  is taken from measurements at the critical point.

After determining  $T_e$  for the current dependent measurements,  $p$  is determined by the gradient of a linear fit to a double log plot of equation (13) as shown in figure 8. The results of all four samples investigated are shown in table 4. Only one transition could be determined in sample L3 owing to lifting of LL spin degeneracy.

To be consistent with the scaling theory of the QHE proposed by Pruisken [6] and the experimental results of Wei *et al* [11], and assuming the universal value of  $\gamma \sim 2.3$ , the value of the temperature exponent is expected to be  $p \sim 2$  irrespective of sample detail or LL index. The values of



**Figure 7.**  $(d\rho_{xy}/dB)_{\max}$  for the  $N = 1 \downarrow$  ( $\nu = 4-3$ ) transition of sample L4 measured as a function of both temperature and current. Temperature-dependent measurements are used as calibration curves for determining  $T_e$  for measurements of different applied currents. The dashed line shows that, as an example, an applied current of 1000 nA is equivalent to  $T_e$  of approximately 600 mK.

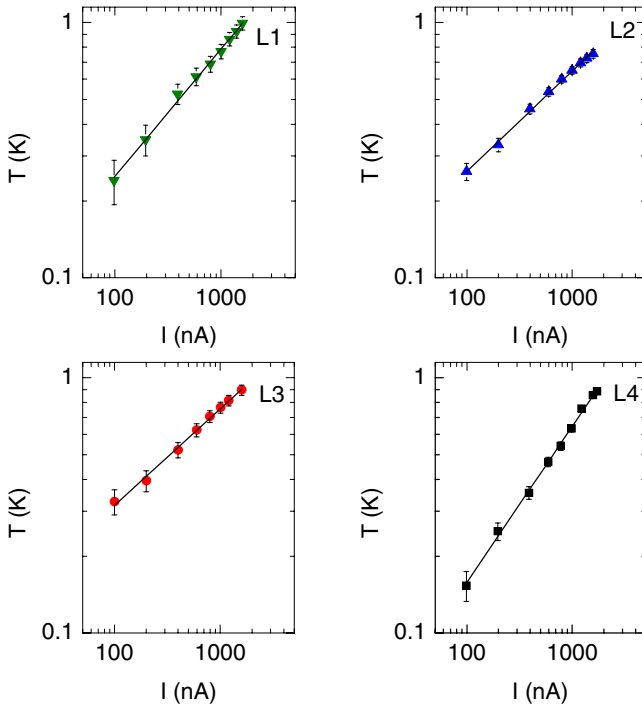


**Figure 8.** Double-log plot of  $T_e$  versus  $I$  for the  $N = 1 \downarrow$  ( $\nu = 4-3$  transition) in all four samples investigated;  $p$  is determined as the gradient of a linear fit to the plot.

$p$  determined in table 4 shows that  $p$  is in fact dependent on sample;  $p$  varies between  $p = 1.27$  and  $p = 3.29$ . The exponent also appears to have a mobility dependence, increasing with decreasing sample mobility. The value of  $p$  has been previously measured by Wei *et al* [26] in InGaAs/InP heterostructures as  $p = 2$  and was declared to be universal, but in investigations on GaAs/AlGaAs heterostructures similar to those used here, Koch *et al* [8] obtained values of  $p$  between  $p = 2.7$  and  $p = 3.4$  using a size-dependent scaling analysis. We find good agreement with Koch *et al* if we limit our results to samples of a similar range of mobilities, obtaining values of  $p$  between  $p = 3.09$  and  $p = 3.29$ . These findings therefore question the universality of  $p$  in GaAs/AlGaAs

**Table 4.** The temperature exponent  $p$  of the phase breaking time measured for various LLs in all four samples:  $N = 1 \downarrow$ ,  $\nu = 4-3$ ;  $N = 2 \uparrow$ ,  $\nu = 5-4$ ;  $N = 2 \downarrow$ ,  $\nu = 6-5$ .

Sample	$N = 1 \downarrow$	$N = 2 \uparrow$	$N = 2 \downarrow$
L1	$2.01 \pm 0.04$	$2.02 \pm 0.08$	$2.06 \pm 0.05$
L2	$3.09 \pm 0.06$	$3.11 \pm 0.13$	$3.23 \pm 0.26$
L3	$3.29 \pm 0.09$	—	—
L4	$1.27 \pm 0.02$	$1.55 \pm 0.09$	$1.64 \pm 0.09$

heterostructures. Figure 9 shows the mobility dependence of  $p$  found in our results by plotting the average value of  $p$  measured in each sample against the sample mobility. It is also noted that at zero magnetic field,  $p$  is predicted to be  $p = 1$  for dirty metals [52], while  $p = 2$  is predicted by Fermi liquid theory for clean metals at zero field [12, 53].

#### 4. Percolation theory of plateau-to-plateau transitions

In this section we discuss the results presented above in the context of a model that describes the interplay between classical percolation and quantum critically in quantum Hall transitions. The percolation model of plateau-to-plateau transitions in the QHE provides an appealing and intuitive picture of Anderson localization that relates localization to classical percolation. By considering quantum tunnelling and interference, the critical behaviour of quantum Hall transitions can be recovered from a classical percolation picture. The percolation model remains one of the most physically transparent models that describes the diversity in experimental data relating to the quantum criticality of PPTs.

The earliest theories of plateau-to-plateau transitions were based on percolation of electron clusters [30, 54], and since then the percolation model has been used extensively to describe the transport properties between quantum Hall plateaux of a 2DES [30, 55–62]. The most popular microscopic view of the IQHE is the edge state picture [63], which suggests that the externally injected current flows exclusively close to the edge of the sample through edge-state

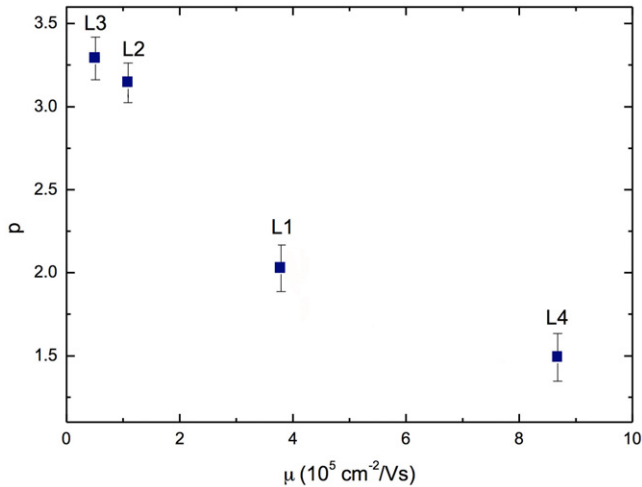


**Figure 9.** Plot showing the dependence of  $p$  on mobility. The values of  $p$  are averaged for each sample and increase with decreasing mobility.

transport [64]. An alternative view describes the integer and fractional QHE through the formation of alternating strips of compressible and incompressible regions [65, 66] within the electron system. Both these descriptions emphasize the role of the edges of the 2DES and involve narrow conducting channels close to the edge of the sample. As a result of advances in scanning techniques that probe the surfaces of electron systems, and provide local electrostatic potential maps, the physical description in the 2DES bulk of isolated and inter-linked clusters has been experimentally observed and verified in several studies [67–73]. In this work, however, we are interested in the conduction through the bulk of the sample at half integer filling factors or PPTs, where both approaches agree with the existence of a percolation-like network of electrons or channel within the bulk of the sample, which then gives rise to a finite dissipative conductivity. It is within this regime that we focus our discussion.

The picture presented here is that in a strong magnetic field and a slowly varying random potential, electrons in a 2DES perform small cyclotron oscillations while the centre of the orbit slowly drift along lines of constant random potential  $V(x, y) = \text{const}$  [30, 60]. These equipotential lines consist of closed trajectories that form potential valleys. Electrons are therefore localized within isolated clusters in the bulk of the 2DES and cannot propagate beyond the boundaries of their clusters. The system therefore exhibits no dissipative current. This is picture found within the localized region of a disorder-broadened LL and is analogous to a classically percolating fluid in random network [74].

As the Fermi energy  $E_F$  moves towards the centre of the LL there is a change in electron density and a redistribution of electrons with respect to the background potential. The electron clusters begin to merge, forming larger clusters with electron trajectories that cover larger distances. At a certain critical energy  $E_c$  close to the centre of the Landau band, clusters merge to form an equipotential line that percolates from one end of the system to the other; this is known as the percolation threshold. An important conclusion drawn from

this description is that since equipotential lines are closed and localized for all energies except the critical energy of the percolation threshold, all electron wave functions must be localized except at the critical energy. This picture provides a clear physical description of the localization length  $\xi_p(E)$ , which can intuitively be observed to be the width of a cluster, or in other words, the maximum displacement of electron belonging to the outmost equipotential of a cluster. According to the classical theory of percolation  $\xi_p(E)$  diverges as the critical energy is approached according to the power law,

$$\xi_p(E) \propto |E - E_c|^{-\gamma_p}, \quad (14)$$

with a universal critical exponent  $\gamma_p = 4/3$  [54] which has been determined exactly [75].

The description above is of a classically percolating system that does not take into account any quantum mechanical effects associated with the disordered Fermi liquid. The inclusion of tunnelling and interference quantum mechanical effects introduces a correction to the percolating electrons at the critical energy and the universal exponent, however. Consider the scenario of two neighbouring clusters within the system as  $E_F$  approaches the centre of a Landau band. Just before the trajectories of the outmost equipotentials of the neighbouring clusters coalesce, an electron is able to tunnel from one cluster to the other at a saddle point of potential between the two clusters. As a result, delocalization of wave functions can occur through saddle points tunnelling, and electrons are no longer localized to one cluster, but can escape to another through the saddle point. It has been shown that this correction to the localization length modifies the critical exponent to a value of  $\gamma = 7/3$  or  $\gamma \approx 2.3$  [30, 55, 56], the expected critical exponent of the quantum phase transition associated with the QHE. The relationship between classical percolation and the QHE has been firmly established in recent numerical and theoretical studies [56, 76–78].

## 5. Discussion

The combined results of the three sets of experiments above suggest an inconsistent and generally non-universal nature of PPTs and the critical exponents involved. This ambiguity in critical exponents associated with PPTs in GaAs/AlGaAs heterostructures has been discussed previously [4], but never before have all the exponents been determined in the same system to reveal a complete picture of criticality both as a function of temperature (quantum coherence length) and magnetic field (energy). Previous explanations of non-universality, especially in GaAs/AlGaAs heterostructures, have been based on partial experimentation and as a result yielded fragmented theories. We present here a broader model of quantum criticality of PPTs that is not only applicable to our results but also to numerous experimental results reported in the literature. The summary of the results above is as follows. (1) An inconsistent picture of quantum criticality is found at around the centre of the Landau band, contrary to previous results [11]. (2) Quantum criticality is conclusively shown to exist in the localized tail regions of the Landau band of

the same measured sample. (3) We find that the temperature exponent  $p$  is not a constant, but it is mobility dependent. The results are discussed below.

We begin with a discussion of universality around the centre of the Landau band. This was determined in our experiments by investigating the temperature dependence of the width of the conductivity peak of a LL to obtain the critical exponent  $\kappa$ . It has previously been argued that the lack of universality arises from the length of correlation of disorder potentials found in the 2DESs investigated [4, 10]. Universal exponents were first reported by Wei *et al* [11, 26] who measured low mobility InGaAs/InP structures, in which short-range random alloy potential scattering dominated. On the other hand, investigation of GaAs/AlGaAs heterostructures [9, 10], in which carrier scattering was dominated by long-range potential fluctuations from remote ionized donors, failed to show the same universal nature of scaling observed in InGaAs/InP structures. Using the percolation model, we describe a broader explanation for this difference.

According to the percolation model described above,  $\kappa$  is determined in a range of the Landau band close to the percolation threshold. As discussed above, it is the inclusion of the quantum mechanical process of saddle point tunnelling that modifies a classically percolating system to a quantum percolating system that possesses quantum criticality. There are two main features underlying the relevance of saddle point tunnelling to quantum criticality. The first is that dissipative transport predominately occurs on the edges of almost touching neighbouring clusters. Wave functions of electrons that propagate on the outmost equipotential trajectory of a cluster, where  $E \sim E_F$ , are linked through quantum tunnelling to the edge of other clusters, forming an extended bulk channel connecting one side of system to the other and enabling dissipative conductivity. It has been shown [56] that contributions to conductivity from electrons with energies that are not too close to the Fermi energy (equipotentials found deep within the cluster) reverts the system to a classically percolating system. Second, the tunnelling process, which causes delocalization of wave functions, enables a quantum coherent extension of the trajectory of an electron beyond the physical dimensions of its isolated cluster. The quantum coherence length  $l_\varphi$ , which represents the dephasing length of wave function beyond which quantum interference terms are suppressed, is no longer limited to the size of the electron cluster as defined by classical percolation. As a result, the crossover between classical percolation and quantum criticality can be expressed as  $l_\varphi = \xi_p$ , where  $\xi_p$  as defined above, represents the size of the typical electron cluster. The system remains classical as long as  $l_\varphi < \xi_p$  but a quantum behaviour and hence quantum critically takes over when  $l_\varphi > \xi_p$ .

The effect of a sufficiently high temperature in this model is to invalidate the two main points discussed above. In the high temperature limit, electrons are able to hop from anywhere within the cluster to an equally arbitrary location within another cluster via phonon induced inelastic scattering. This is essentially the onset of transport via thermal activation. As a result of the activation process, dissipative conductivity

is no longer dominated by electrons near  $E_F$ . In addition, an increase in temperature causes a decrease in  $l_\varphi(T)$  such that at a high enough temperature the condition  $l_\varphi < \xi_p$  is reached. With such a short dephasing length an electron is scattered before it is able to escape its cluster through a saddle point. There is therefore no quantum coherent extension of the localization length or quantum interference between clusters and the system reverts to a classical percolation system.

Since the experimental results reported here on exponent  $\kappa$  deviates for the expected quantum critical value, following from the discussion above, it must mean that least some section of the temperature range of our experiments is found within the classical  $l_\varphi < \xi_p$  regime and thus the determined values for  $\kappa$  will overlap both the quantum critical and classical region.  $\kappa$  in this case will be a mixture of both exponents with a value between the quantum critical  $\kappa = 0.42$  and the classical  $\kappa = 0.75$ . We believe that this is the reason why so many previous experimental investigations report different values for the critical exponent which typical ranges between 0.42 and 0.75. The quantum–classical crossover point itself is not observed in our results due to the low resolution in temperature of the data taken, although we have experimentally observed the crossover point using a high resolution frequency scaling technique that allows  $l_\varphi$  to be varied with finer granularity on similar GaAs/AlGaAs heterostructures [79]. We therefore conclude that although quantum criticality must exist in our samples as demonstrated by results in the tail regions of the LL, we suspect that at the centre of the LL lower temperatures than can be obtained in our experiments are needed in order to observe the quantum criticality at the correct value of the critical exponent.

One consequence of the crossover proposed by the percolation model presented here on the quantum criticality of  $\kappa$  is the importance of the typical cluster size close to the percolation threshold. It is noted that since the quantum mechanical behaviour of the system is only valid when  $l_\varphi > \xi_p$ , there is a greater chance of observing quantum criticality in system where  $\xi_p$  is smaller. Since  $\xi_p$  denotes the width of the typical cluster, this can be achieved by increasing the background disorder potentials to create smaller fragments of electron clusters. We have observed this disorder induced crossover in GaAs/AlGaAs heterostructures where the background disorder potential was increased by introducing Al impurities in the vicinity of the 2DES [27]. It was shown that by increasing the disorder within the system, quantum criticality can be observed in an otherwise non-universal GaAs/AlGaAs heterostructure. The relationship between cluster size and the quantum critical-to-classical percolation crossover of  $\kappa$  is even more convincingly established in recent experimental results reported by Li *et al* [80].

We attribute this interplay between cluster size and quantum coherence length to be the reason for the experimentally observed difference between short-range disordered systems and long-range disordered systems. In InGaAs/InP heterostructures where disorder within the system is due to short-range alloy scattering, typical cluster sizes are intuitively expected to be smaller owing to the relatively strong background disorder potential compared to GaAs/AlGaAs

structures. Disorder in GaAs/AlGaAs systems on the other hand originates from long-range potential fluctuation from ionized impurities that are separated from the 2DES by a spacer layer. This cuts off the core of the Coulomb potential, leaving the 2DES to experience only the weak interaction in the tails [81]. This produces cluster sizes that are typically larger than those found in InGaAs/InP systems. Due to this relative difference in cluster sizes, quantum criticality, which as described above is observed when  $l_\varphi > \xi_p$ , is found at a lower temperature in GaAs/AlGaAs systems than in InGaAs/InP. This requires experiments on GaAs/AlGaAs systems to probe a much lower range of temperature to observe quantum criticality. Indeed, it has been shown that by progressively changing the background potential in a typical GaAs/AlGaAs heterostructures, the crossover point can be shifted towards higher temperatures, revealing the quantum critical region [80].

We now discuss criticality within the tail regions of the LL band, and the critical exponent  $\gamma$ , which is determined within this region. It was argued above that the observation of quantum criticality relied on the existence of quantum mechanical processes, specifically quantum tunnelling of electrons at the Fermi energy through saddle points that, in turn, extend the quantum coherence trajectories beyond individual clusters. This picture is valid close to the percolation threshold where these saddle points are most likely to occur. In the tail regions, however, localization is characterized by clusters that are close in energy but with localization lengths that are small compared with the spatial distance between the centres of clusters. In other words, the spatial distance between clusters is much larger than that found close to the percolation threshold, and thus there are diminishing numbers of saddle points. At sufficiently low temperatures, transport in this regime is dominated by states whose energies are concentrated in a narrow band near the Fermi level [35, 36]. In the absence of saddle points an electron is likely to tunnel longer distances to reach sites that minimize the energy requirement for transport (i.e. the variable range hopping regime). In other words, as one moves away from the centre of the Landau band, saddle point-like tunnelling between the outmost equipotential trajectories of clusters is still maintained via VRH. The two requirements for observing quantum criticality are still maintained; transport is still dominated by electrons at the Fermi level, and there is a quantum coherent extension of the coherence length beyond the size of the cluster.

This form of transport is quantum coherent as long as the quantum coherence length is larger than the localization length [82],  $l_\varphi > \xi$ , and since  $\xi$  is exponentially small in the tails of the LL band, VRH is more temperature robust than saddle point tunnelling and thus persists for a higher range of temperatures. This is the reason why even though we do not observe quantum criticality at the centre of the LL in the results presented in this paper, it is observed in the tail regions of the LL of the same sample in the data presented above. At a sufficiently high temperature though there is a breakdown of VRH and a thermally activated process takes over. The onset of the activated process is in fact seen in the high field determination of  $\gamma$  in sample L3 (table 2) where the measured value of the

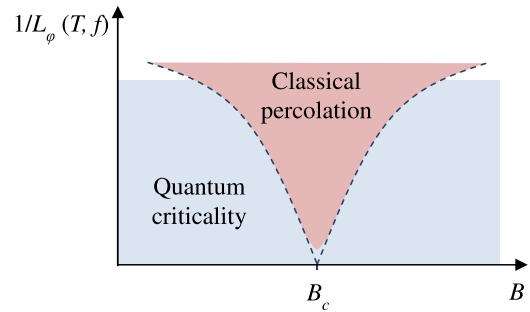


**Figure 10.** A diagrammatic representation of the criticality of plateau-to-plateau transitions across a LL band.

critical exponent tends towards the classically expected value of  $\gamma \approx 1.3$ . Investigations of the critical exponent carried out in the tail regions of a LL band by Zhao *et al* [83] have indeed confirmed that  $\gamma$  takes on the classical value of  $\gamma \approx 1.3$  in the activated transport regime.

A summary of our experimental results can be described by the criticality diagram shown in figure 10. The basic idea of the schematic, which is supported both by the percolation model and by observed experimental results, is that there is a breakdown of the quantum critical nature of PPTs at sufficiently high temperatures.

The dashed line in figure 10 denotes the boundary of the quantum–classical crossover of criticality. As discussed above, an increase temperature results in a decrease in  $l_\varphi$ . In the tail regions of the Landau band quantum criticality is observed but in the high temperature limit the onset of activated processes of conduction causes a crossover from quantum criticality to classical percolation as observed in our results.

At the centre of the Landau band, however, the schematic shows that quantum criticality is observed within a narrow range of temperatures after which there is a crossover to classical behaviour. The difference in robustness of the observation of quantum criticality between the tail region and the centre of the band is due to the difference in the cluster size within these regions and the requirement for a quantum coherent extension of the  $l_\varphi$  beyond the cluster size. Since the size of the clusters are smaller in the tail regions this requirement is invalidated at higher temperatures but due to larger cluster sizes at the centre of the band, the requirement is even invalidated at relatively lower temperatures.

We note that a similar picture has been predicted by Kapitulnik *et al* [59], where it was used to explain superconductor-to-insulator transitions, but it clear that the same idea is applicable to our experiments and to plateau-to-plateau transitions.

The final set of experiments presented here is based on the determination of the inelastic scattering length exponent  $p$  where it is assumed that  $p = 2$  in most quantum criticality experiments. An interesting feature that we observe is the apparent mobility dependence of  $p$ . Although a similar method using electron heating was employed on InGaAs/InP heterostructures, the nature of disorder in these samples was short-range and the expected universal value of  $p = 2$  was obtained [26]. The results obtained in the short-range disorder

InGaAs/InP samples cannot be directly compared to the long-range disordered GaAs/AlGaAs system since it has become clear that the range of the disorder potential plays an important role in the scaling theory of the QHE. Previous investigations of  $p$ , which have been based on size-dependent experiments, agree with our results from the electron heating method. In these size-dependent experiments, the expected universality was found in short-range disorder systems [33], but not in long-range systems [8]. Comparing results from like-for-like heterostructures, our electron heating results agree well with the size-dependent results. It is not obvious though from the size-dependent results that  $p$  has a mobility dependence, because of the narrow range of samples and mobilities considered previously. It should be noted that had we considered the same range of mobilities too, the apparent mobility dependence would also not be evident.

In summary, our data leads us to conclude that classical transport around the LL critical point affects the determination of  $p$  in GaAs/AlGaAs heterostructures with long-range disorder.

## 6. Conclusions

We offer a unifying picture of quantum criticality in 2DESs where we are able to draw conclusions based on experimental observations with the aid of a percolation model. By measuring all critical exponents in the same sample, we are able to make deductions based on our observations of quantum criticality in long-range disordered systems. We conclude that quantum criticality does indeed exist in long-range systems but is more difficult to observe at the centre of the LL bands owing to the interplay between cluster size and the quantum coherence length. We also find an unexpected mobility dependence on  $p$ , which awaits further theoretical analysis.

## Acknowledgment

We are grateful for the support of the EPSRC, the Royal Society, the Wolfson Foundation and the ERC programme, NOTES.

## References

- [1] Halperin B I 1982 *Phys. Rev. B* **25** 2185
- [2] Klitzing K v, Dorda G and Pepper M 1980 *Phys. Rev. Lett.* **45** 494
- [3] Sondhi S *et al* 1997 *Rev. Mod. Phys.* **69** 315
- [4] Huckestein B 1995 *Rev. Mod. Phys.* **67** 357
- [5] Aoki H and Ando T 1985 *Phys. Rev. Lett.* **54** 831
- [6] Pruisken 1988 *Phys. Rev. Lett.* **61** 1297
- [7] Thouless D J 1977 *Phys. Rev. Lett.* **39** 1167
- [8] Koch S *et al* 1991 *Phys. Rev. Lett.* **67** 883
- [9] Koch S *et al* *Phys. Rev. B* **43** 6828
- [10] Wei H P *et al* 1992 *Phys. Rev. B* **45** 3926
- [11] Wei H P *et al* 1988 *Phys. Rev. Lett.* **61** 1294
- [12] Huckestein B and Kramer B 1990 *Phys. Rev. Lett.* **64** 1437
- [13] Huckestein B, Kramer B and Schweitzer L 1992 *Surf. Sci.* **263** 125
- [14] Hohls F, Zeitler U and Haug R J 2002 *Phys. Rev. Lett.* **88** 036802
- [15] Hohls F, Zeitler U and Haug R J 2001 *Phys. Rev. Lett.* **86** 5124
- [16] Hohls F *et al* 2002 *Phys. Rev. Lett.* **89** 276801
- [17] Balaban N Q, Meirav U and Bar-Joseph I 1998 *Phys. Rev. Lett.* **81** 4967
- [18] Das Sarma S and Liu D 1993 *Phys. Rev. B* **48** 9166
- [19] Shashkin A A, Dolgoplov V T and Kravchenko G V 1994 *Phys. Rev. B* **49** 14486
- [20] Shahar D *et al* 1998 *Solid State Commun.* **107** 19
- [21] Kuchar F *et al* 2000 *Europhys. Lett.* **49** 480
- [22] Ruzin I M, Cooper N R and Halperin B I 1996 *Phys. Rev. B* **53** 1558
- [23] Koch S *et al* 1995 *Semicond. Sci. Technol.* **10** 209
- [24] Hwang S W *et al* 1993 *Phys. Rev. B* **48** 11416
- [25] Furlan M 1998 *Phys. Rev. B* **57** 14818
- [26] Wei H P, Engel L W and Tsui D C 1994 *Phys. Rev. B* **50** 14609
- [27] Saeed K *et al* 2011 *Phys. Rev. B* **84** 155324
- [28] Li W *et al* 2005 *Phys. Rev. Lett.* **94** 206807
- [29] Mott N F and Davis E A 1971 *Electronic Processes in Non-Crystalline Materials* (Oxford: Clarendon)
- [30] Chalker J and Coddington P 1988 *J. Phys. C: Solid State Phys.* **21** 2665
- [31] Lee D K K and Chalker J T 1994 *Phys. Rev. Lett.* **72** 1510
- [32] Huo Y and Bhatt R N 1992 *Phys. Rev. Lett.* **68** 1375
- [33] Li W *et al* 2009 *Phys. Rev. Lett.* **102** 216801
- [34] Polyakov D G and Shklovskii B I 1993 *Phys. Rev. Lett.* **70** 3796
- [35] Mott N F 1968 *J. Non-Cryst. Solids* **1** 1
- [36] Efros A and Shklovskii B 1975 *J. Phys. C: Solid State Phys.* **8** L49
- [37] Briggs A *et al* 1983 *Phys. Rev. B* **27** 6549
- [38] Van Keuls F W *et al* 1997 *Phys. Rev. B* **56** 1161
- [39] Ebert G *et al* 1983 *Solid State Commun.* **45** 625
- [40] Ono Y 1982 *J. Phys. Soc. Japan* **51** 237
- [41] Jiang H W *et al* 1993 *Phys. Rev. Lett.* **71** 1439
- [42] Engel L W *et al* 1993 *Phys. Rev. Lett.* **71** 2638
- [43] Wakabayashi J *et al* 1992 *J. Phys. Soc. Japan* **61** 1691
- [44] Wakabayashi J *et al* 1990 *Surf. Sci.* **229** 60
- [45] Anderson P W, Abrahams E and Ramakrishnan T V 1979 *Phys. Rev. Lett.* **43** 718
- [46] Uren M J *et al* 1981 *J. Phys. C: Solid State Phys.* **14** L395
- [47] Fang F 1970 *J. Appl. Phys.* **41** 1825
- [48] Polyakov D G and Shklovskii B I 1993 *Phys. Rev. B* **48** 11167
- [49] Neugebauer T and Landwehr G 1980 *Phys. Rev. B* **21** 702
- [50] Hirakawa K and Sakaki H 1986 *Appl. Phys. Lett.* **49** 889
- [51] Manion S J *et al* 1987 *Phys. Rev. B* **35** 9203
- [52] Altshuler B L *et al* 1982 *J. Phys. C: Solid State Phys.* **15** 7367
- [53] Huckestein B 1992 *Europhys. Lett.* **20** 451
- [54] Trugman S A 1983 *Phys. Rev. B* **27** 7539
- [55] Dubi Y, Meir Y and Avishai Y 2005 *Phys. Rev. Lett.* **94** 156406
- [56] Dubi Y, Meir Y and Avishai Y 2005 *Phys. Rev. B* **71** 125311
- [57] Lee D-H, Wang Z and Kivelson S 1993 *Phys. Rev. Lett.* **70** 4130
- [58] Chklovskii D B and Lee P A 1993 *Phys. Rev. B* **48** 18060
- [59] Kapitulnik A *et al* 2001 *Phys. Rev. B* **63** 125322
- [60] Kramer B, Ohtsuki T and Kettemann S 2005 *Phys. Rep.* **417** 211
- [61] Shimshoni E and Auerbach A 1997 *Phys. Rev. B* **55** 9817
- [62] Shimshoni E, Auerbach A and Kapitulnik A 1998 *Phys. Rev. Lett.* **80** 3352
- [63] Büttiker M 1988 *Phys. Rev. B* **38** 9375
- [64] Haug R J 1993 *Semicond. Sci. Technol.* **8** 131
- [65] Beenakker C W J 1990 *Phys. Rev. Lett.* **64** 216
- [66] Chang A M 1990 *Solid State Commun.* **74** 871
- [67] Hashimoto K *et al* 2008 *Phys. Rev. Lett.* **101** 256802

- [68] Hashimoto K *et al* 2011 *J. Phys.: Conf. Ser.* **334** 012008  
[69] Tessmer S H *et al* 1998 *Nature* **392** 51  
[70] Eytan G *et al* 1998 *Phys. Rev. Lett.* **81** 1666  
[71] Zhitenev N B *et al* 2000 *Nature* **404** 473  
[72] Ilani S *et al* 2004 *Nature* **427** 328  
[73] Baumgartner A *et al* 2007 *Phys. Rev. B* **76** 085316  
[74] Stauffer D 1979 *Phys. Rep.* **54** 1  
[75] Saleur H and Duplantier B 1987 *Phys. Rev. Lett.* **58** 2325  
[76] Schubert G and Fehske H 2008 *Phys. Rev. B* **78** 155115  
[77] Sandler N, Maei H R and Kondev J 2004 *Phys. Rev. B* **70** 045309  
[78] Beamond E J, Cardy J and Chalker J T 2002 *Phys. Rev. B* **65** 214301  
[79] Dodoo-Amoo N A *et al* 2014 unpublished  
[80] Li W *et al* 2010 *Phys. Rev. B* **81** 033305  
[81] Nixon J A and Davies J H 1990 *Phys. Rev. B* **41** 7929  
[82] E. Shimshoni 1999 *Phys. Rev. B* **60** 10691  
[83] Zhao Y J *et al* 2008 *Phys. Rev. B* **78** 233301